JVI Journals.ASM.org

The Rigid Amphipathic Fusion Inhibitor dUY11 Acts through Photosensitization of Viruses

Frederic Vigant,[a] Axel Hollmann,[b] Jihye Lee,[c] Nuno C. Santos,[b] Michael E. Jung,[c] Benhur Lee[a]

Department of Microbiology, Immunology and Molecular Genetics, University of California Los Angeles, Los Angeles, California, USA[a]; Instituto de Medicina Molecular, Faculdade de Medicina, Universidade de Lisboa, Lisbon, Portugal[b]; Department of Chemistry and Biochemistry, University of California Los Angeles, Los Angeles, California, USA[c]

Rigid amphipathic fusion inhibitors (RAFIs) are lipophilic inverted-cone-shaped molecules thought to antagonize the membrane curvature transitions that occur during virus-cell fusion and are broad-spectrum antivirals against enveloped viruses (Broad-SAVE). Here, we show that RAFIs act like membrane-binding photosensitizers: their antiviral effect is dependent on light and the generation of singlet oxygen ($^1O_2$), similar to the mechanistic paradigm established for LJ001, a chemically unrelated class of Broad-SAVE. Photosensitization of viral membranes is a common mechanism that underlies these Broad-SAVE.

Recently, a few broad-spectrum antivirals have been described that target enveloped virus entry (1–10). Antivirals that can target the biophysical process of virus-cell membrane fusion itself, rather than any particular viral protein, not only have the potential to be truly broad spectrum (against any enveloped virus) but also will likely have a high barrier to resistance (11–14). Thus, gaining a fuller mechanistic understanding of antiviral compounds reported to target the virus-cell membrane fusion process is essential for developing the potential of this exciting broad-spectrum antiviral strategy.

We originally described a class of thiazolidine-based lipophilic broad-spectrum antivirals against enveloped viruses (Broad-SAVE) (e.g., LJ001) that target a late stage of virus-cell fusion at the level of membrane merger (9). Follow-up studies indicated that LJ001, our first generation of Broad-SAVE, and the oxazolidine-based JL series of compounds, our second generation Broad-SAVE, act as membrane-targeted photosensitizers: they generate singlet oxygen ($^1O_2$) in the plane of the membrane, and $^1O_2$-mediated lipid oxidation results in changes in the biophysical properties of the viral envelope that are not conducive to virus-cell membrane fusion (8). The salient point is that at antiviral concentrations, $^1O_2$-mediated lipid oxidation is not detrimental to metabolically active cell membranes. This is the key mechanistic paradigm that has never been explicitly stated and tested (15) until our recent studies (8, 9).

Shortly after our original description of the membrane-targeted broad-spectrum antiviral LJ001 (9), St. Vincent et al. de-

Received 21 October 2013 Accepted 20 November 2013
Published ahead of print 27 November 2013
Address correspondence to Benhur Lee, bleebhl@ucla.edu.
A.H. and J.L. contributed equally.
Supplemental material for this article may be found at http://dx.doi.org/10.1128/JVI.02907-13.

doi:10.1128/JVI.02907-13

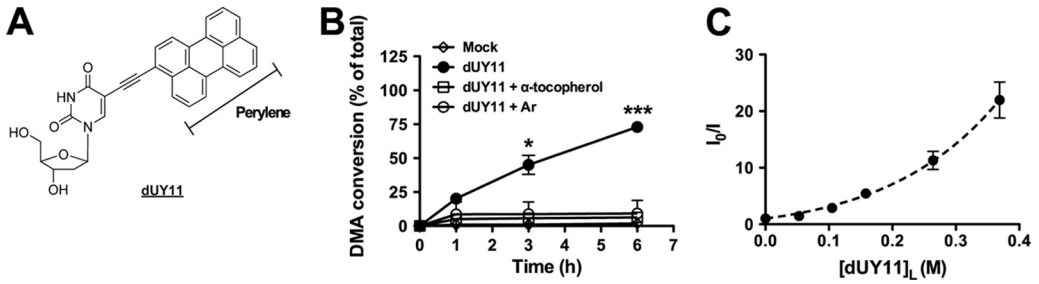

FIG 1 dUY11 generates singlet oxygen ($^1O_2$). (A) Structure of dUY11 and its perylene core. (B) dUY11 was added to a solution of 9,10-dimethylanthracene (DMA) and exposed to light. At 0.1, 1, 3, or 6 h, DMA conversion was detected by ^{1}H-nuclear magnetic resonance (NMR) (DMA/oxiDMA = 3.1 ppm:2.1 ppm [methyl peak]). Reactions were performed in tetrahydrofuran (THF) using 1 equivalent of DMA and 0.5 equivalent of dUY11, and α-tocopherol where applicable, under an O_2 atmosphere. Where applicable, THF was purged with argon (Ar) by the freeze-thaw method before the reaction was performed under Ar atmosphere. Mean ± standard deviation (SD), $n = 2$ independent measurements. *, $P < 0.05$; ***, $P < 0.001$, two-way analysis of variance (ANOVA) followed by a Bonferroni posttest for multiple comparisons. (C) DMA conversion by $^1O_2$ production in 3 mM POPC (a C9 monounsaturated model phospholipid) LUV. It should be noted that concentrations indicated in POPC are the local concentration of dUY11 in the strict lipid bilayer volume, calculated as described in reference 25. $^1O_2$ production was measured through its effect on a fluorescent $^1O_2$ chemical trap. DMA reacts selectively with $^1O_2$ in membranes to form the nonfluorescent 9,10-endoperoxide ($DMAO_2$). By monitoring the disappearance of DMA's fluorescence signal (excitation at 379 nm and emission at 432 nm), we were able to estimate the level of $^1O_2$ in the membrane. $^1O_2$-associated fluorescence disappearance data were analyzed using the quenching sphere-of-action model, $I_0/I = 1 + K^*_{sv}[Q]e^{VN_A[Q]}$, where K^*_{sv} is the apparent Stern-Volmer constant (indicating the reduction of fluorescence by the conversion of DMA to $DMAO_2$), V is the sphere-of-action volume (i.e., the sphere that surrounds the chromophore within which the "quencher" can be considered to be in contact with the chromophore), and N_A is Avogadro's constant. Mean ± SD, $n = 3$ independent measurements.

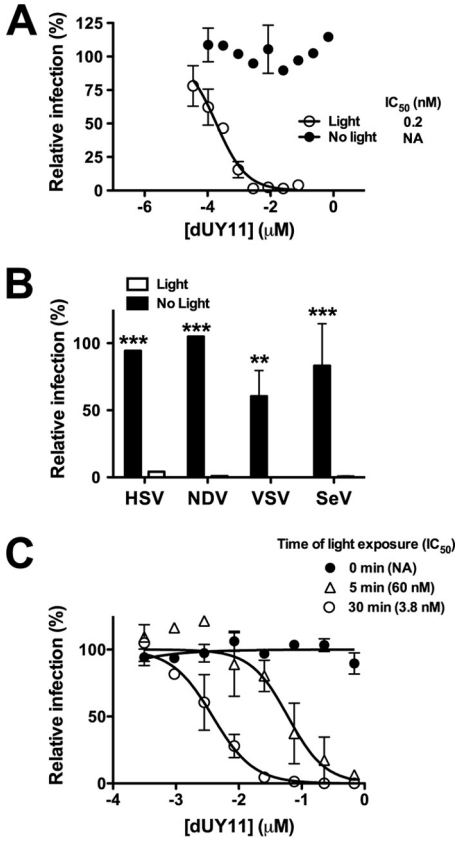

FIG 2 dUY11's antiviral activity is dependent on light. (A) Dose-response of dUY11 against HSV-1–GFP, in the presence (10 min) or absence of light, analyzed by flow cytometry. Mean ± SD, $n = 2$ biological replicates. NA, not active. (B) Antiviral activity of 1 μM dUY11 against HSV-1–GFP, NDV-GFP, VSV-Luc, and SeV-GFP in the presence (10 min) or absence of light, analyzed by flow cytometry (GFP) or luciferase activity in cell lysates (Luc). Mean ± SD, $n = 2$ biological replicates. Light versus no light: **, $P < 0.01$; ***, $P < 0.001$, two-way ANOVA followed by a Bonferroni posttest for multiple comparisons. (C) Dose-response antiviral activity (IC_{50}) of dUY11 against NDV-GFP under various times of light exposure (0, 5, and 30 min), analyzed by flow cytometry. Mean ± SD, $n = 2$ biological replicates. IC_{50} values were calculated using nonlinear regression analysis in GraphPad Prism. All data are presented as relative percentages of infection normalized to mock-treated conditions (set as 100%). Five minutes versus 30 min of light exposure, $P < 0.0001$, extra sum-of-squares F-test.

scribed another class of antiviral molecules termed rigid amphipathic fusion inhibitors (RAFIs) that also inhibit a number of enveloped viruses at the level of virus-cell fusion (6). Mechanistic studies indicate that RAFIs have "remarkably similar properties" to LJ001. However, the authors present evidence that these RAFIs inhibit virus-cell fusion by stabilizing the positive curvature of membranes by virtue of their molecular geometry: RAFIs are inverted-cone-shaped molecules with a large hydrophilic head group attached to a rigid and planar hydrophobic moiety that inserts into the membrane. Thus, RAFIs are thought to act like similarly shaped lysophospholipids, which are known to impair the critical positive-to-negative membrane transitions that occur during virus-cell fusion (2, 7). Nevertheless, we noted that the rigid and planar hydrophobic moiety present in all effective RAFIs is a perylene group (Fig. 1A) (3, 6), which is a well-known fluorescent lipid probe and photosensitizer (16–18).

We, and others, have previously questioned whether the nanomolar potency and apparent irreversible antiviral activity of RAFIs can be attributed entirely to their molecular geometry (11, 13). Thus, we synthesized the exemplar RAFI compound, dUY11 (see the supplemental material and Fig. 1A), and asked if dUY11 is a photosensitizer and, if so, whether its ability to generate $^1O_2$ does contribute to its antiviral activity (13).

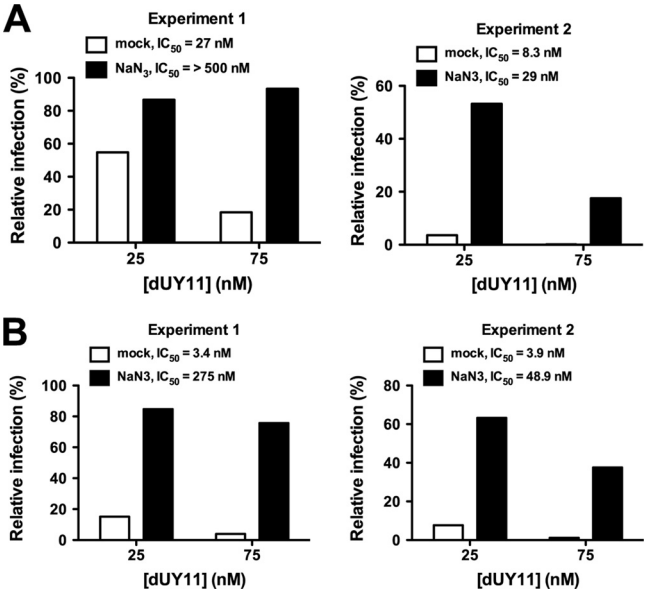

FIG 3 dUY11's antiviral activity is dependent on $^1O_2$. Antiviral activity of 25 and 75 nM dUY11 in the absence (mock) or presence of 100 mM of the specific $^1O_2$ quencher NaN_3. (A) HSV-1–GFP; (B) NDV-GFP. Infection was analyzed by flow cytometry, and data are presented as relative percentages of infection normalized to percentages of GFP-positive cells observed under mock-treated conditions (set as 100%).

Indeed, dUY11 generated $^1O_2$ in solution, as indicated by the oxidation of the $^1O_2$-specific trap 9,10-dimethylanthracene (DMA) (8) (Fig. 1B). Anaerobic conditions (argon [Ar]) or addition of an antioxidant (α-tocopherol) abrogated dUY11-induced DMA oxidation, underscoring the specificity of these results. DMA is lipophilic and highly fluorescent when intercalated into membranes. DMA fluorescence quenching analysis upon oxidation by dUY11 in 1-palmitoyl-2-oleoyl-sn-glycero-3-phosphocholine (POPC) large unilamellar vesicles (LUV) further confirmed the ability of dUY11 to generate $^1O_2$ in membranes (Fig. 1C) and established dUY11 as a type II photosensitizer (19).

Next, to determine if the photosensitizing properties of dUY11 contributed to its antiviral activity, we performed dose-response experiments in the presence or absence of light, as previously described (8). Human herpes simplex virus 1 (HSV-1), a virus extensively used to characterize the antiviral activity of RAFIs, was preincubated with various concentrations of dUY11 for 30 min in the absence of light and then either exposed to a white-light source for an additional 10 min or not, before being used to infect Vero cells. Infectivity analysis confirmed that dUY11 was as potent against HSV-1 (0.2 nM 50% inhibitory concentration [IC_{50}]) (Fig. 2A) and as nontoxic (1.5 mM 50% cytotoxic concentration [CC_{50}]) (data not shown) as previously reported (3, 6). However, dUY11 showed a complete absence of antiviral activity when no light was provided (Fig. 2A), even at concentrations 100-fold above the reported IC_{50} for dUY11 (3, 6). Similar results were obtained using various enveloped RNA viruses unrelated to

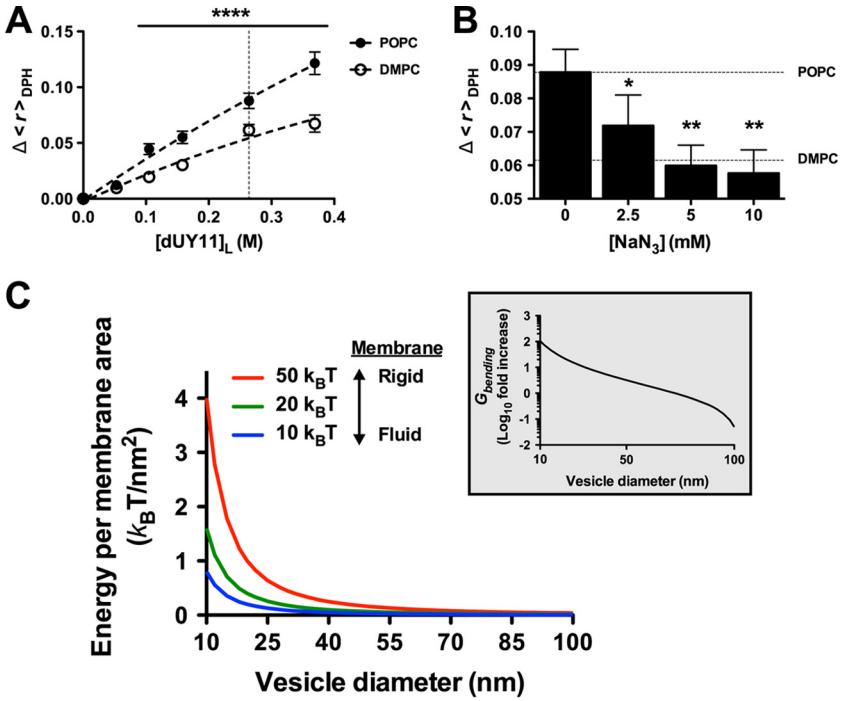

FIG 4 dUY11 increases membrane rigidity through generation of $^1O_2$. (A) Effects of dUY11 on membrane rigidity measured by DPH fluorescence anisotropy changes ($\Delta<r>_{DPH}$), in saturated (DMPC) or unsaturated (POPC) phospholipid LUV, at 37°C. $[dUY11]_L$ (*x* axis) refers to the final concentration in the membranes (lipid bilayer volume) (25). $n = 3$ or 4 independent measurements. ****, $P < 0.0001$, two-way ANOVA followed by a Bonferroni posttest for multiple comparisons. (B) Effects of increasing concentrations of the $^1O_2$ quencher NaN_3 on the anisotropy value change induced by the addition of dUY11 to POPC LUV at 37°C, $[dUY11]_L = 264$ nM (vertical dashed line in panel A). Horizontal dashed lines in panel B correspond to the $\Delta<r>_{DPH}$ values determined without NaN_3, in POPC and DMPC LUV. Anisotropy determinations were made at 37°C, far above the gel- to liquid-phase transition temperatures (T_m) of DMPC and POPC, in order to guarantee that both lipid systems are in the liquid crystalline phase with similar DPH anisotropy values (≈0.065 ± 0.005). $n = 3$ or 4 independent measurements. *, $P < 0.05$; **, $P < 0.01$, one-way ANOVA followed by a Dunnett posttest for multiple comparisons versus the control column ($NaN_3 = 0$ mM). (C) $G_{bending}$ can be defined in energy units, k_BT (where k_B is the Boltzmann's constant and T the absolute temperature). This membrane bending force ranges from 10 k_BT (for highly fluid membranes, blue line) to 50 k_BT (for less fluid membranes with 50% cholesterol, red line) (26, 27), the latter being similar to the plasma membranes of mammalian cells. For any given membrane rigidity (blue, green, and red lines), note the exponential increase in absolute energy required (k_BT/nm^2) for bending membranes as the vesicle diameter gets smaller. The inset shows a specific simulation where a 5% increase in membrane rigidity (50→55 k_BT) on a 100-nm-sized vesicle (virion) results in at least a 3-log increase in energy required to reach the estimated diameter of the fusion stalk (10 nm). The actual energy cost is likely much higher, as the model assumes bending from an initially flat membrane, whereas fusion requires bending from a positively curved to a negatively curved membrane.

HSV-1 (a DNA virus), such as Newcastle disease virus (NDV), Sendai virus (SeV), and vesicular stomatitis virus (VSV) (Fig. 2B), confirming that the broad-spectrum antiviral activity of dUY11 against enveloped viruses is indeed light dependent. As a type II photosensitizer, dUY11's antiviral activity should be dependent on both its concentration and the time of light exposure. Indeed, using NDV-green fluorescent protein (GFP), we found that the antiviral activity of dUY11 increased (lower IC_{50}) as a function of the time of light exposure (Fig. 2C), similar to what has been described for LJ001 (8).

Finally, sodium azide (NaN_3), a specific quencher of $^1O_2$ (20), reversed the antiviral activity of dUY11 against HSV-1 and NDV (Fig. 3A and B, respectively). Note that the apparent potency of dUY11 against both viruses was greater in experiment 2 (lower IC_{50}), concordant with the lesser degree of NaN_3-mediated reversal observed, especially at higher concentrations (75 nM) of dUY11. In sum, our results confirm the specific involvement of $^1O_2$ in dUY11's broad-spectrum antiviral activity.

$^1O_2$-mediated lipid oxidation targets the C=C double bonds in unsaturated phospholipids and introduces polar hydroxylated acyl chains in the middle of the hydrophobic membrane lipid bilayer. Clustering of these oxidized phospholipids results in decreased membrane fluidity, which negatively impacts on the membrane's ability to undergo the extreme membrane curvature transitions occurring during virus-cell fusion (8, 21). Thus, photosensitization of viral membranes requires the presence of unsaturated acyl chains and results in a decrease in membrane fluidity or increased rigidity. To determine if dUY11 induced such biophysical changes in model membranes, we measured the fluorescence anisotropy of the 1,6-diphenyl-1,3,5-hexatriene (DPH) probe after treatment of artificial membranes with dUY11. In Fig. 4A, the dose-dependent increase in anisotropy ($\Delta<r>_{DPH}$), mediated by dUY11, reflected its effect on increasing membrane rigidity (22). Furthermore, the anisotropy increase was more prominent in unsaturated (POPC) than saturated (dimyristoylphosphatidylcholine [DMPC]) phospholipid LUV (Fig. 4A), consistent with the specific targeting of unsaturated phospholipids by dUY11-induced $^1O_2$. The latter was confirmed by the addition of the $^1O_2$ quencher NaN_3, which brought the anisotropy levels of dUY11-treated POPC LUV back to the background levels observed with DMPC LUV (Fig. 4B).

Thus, we propose a mechanism of action for the exemplar RAFI, dUY11, that is similar to the membrane-targeting photosensitizers previously described as Broad-SAVE, such as LJ001 (9)

and its oxazolidine counterparts (e.g., JL103, JL118, and JL122) (8). Our model is consistent with all published data on RAFIs, including those regarding membrane fluidity and lipid-phase transitions of model membranes (3, 6). In contrast, the purely geometric mechanism proposed by Schang and colleagues (stabilization of positive curvature) (3, 6) cannot explain the light dependency of dUY11's antiviral activity or the reversal of its antiviral activity by the $^1O_2$ quencher NaN_3. dUY11 (RAFIs) could very well stabilize positive membrane curvature at high molar concentrations; however, this effect is unlikely to contribute to the antiviral effect seen at its nanomolar IC_{50}.

Recently, Stachowiak and colleagues provided a lucid accounting of the energetics involved in membrane curvature (21). The energy cost per membrane area of creating a curved sphere was estimated as $G_{\text{bending}} = (8\pi\kappa)/(4\pi r^2)$, where κ is the bending rigidity of the membrane and r is the vesicle radius. The bending rigidity ranges from 10 k_BT for a highly fluid membrane with unsaturated phospholipids to 50 k_BT for plasma (or plasma-like) membranes containing 50% cholesterol, where k_B is the Boltzmann's constant and T the absolute temperature. The bending energetics model suggests that even a small increase in bending rigidity, when coupled to a large decrease in vesicle radius (such as the diameter of the fusion stalk during hemifusion), can result in an exponentially insurmountable amount of energy required to bend the membranes for productive fusion to occur (Fig. 4C).

In conclusion, since all the active RAFIs described to date (3, 6) possess a perylene core, it is likely that their antiviral activity is effectuated through the photosensitizing mechanism of action proposed for dUY11 (13). Our data underscore the generalizability and relevance of our recently proposed mechanism of action for Broad-SAVE that target the lipid component of membrane fusion (8). Although the clinical potential of photoactivated membrane-targeting Broad-SAVE appears limited by photophysical hurdles, structure-activity relationship (SAR) studies that leverage advances in photochemistry and nanotechnology may overcome these hurdles (23, 24). The unique mechanism of action of these Broad-SAVE warrants further investigation.

ACKNOWLEDGMENTS

This work was supported by NIH grants U01 AI070495, U01 AI082100, R01 AI069317, and U54 AI065359 (PSWRCE) (to B.L.) and by Fundação para a Ciência e a Tecnologia—Ministério da Educação e Ciência (Portugal) project DELIN—HIVERA/0002/2013 and fellowship SFRH/BPD/72037/2010 (to N.C.S. and A.H., respectively).

REFERENCES

1. **Cheng G, Montero A, Gastaminza P, Whitten-Bauer C, Wieland SF, Isogawa M, Fredericksen B, Selvarajah S, Gallay PA, Ghadiri MR, Chisari FV.** 2008. A virocidal amphipathic {alpha}-helical peptide that inhibits hepatitis C virus infection in vitro. Proc. Natl. Acad. Sci. U. S. A. **105:**3088–3093. http://dx.doi.org/10.1073/pnas.0712380105.
2. **Chernomordik LV, Vogel SS, Sokoloff A, Onaran HO, Leikina EA, Zimmerberg J.** 1993. Lysolipids reversibly inhibit Ca(2+)-, GTP- and pH-dependent fusion of biological membranes. FEBS Lett. **318:**71–76. http://dx.doi.org/10.1016/0014-5793(93)81330-3.
3. **Colpitts CC, Ustinov AV, Epand RF, Epand RM, Korshun VA, Schang LM.** 2013. 5-(Perylen-3-yl)ethynyl-arabino-uridine (aUY11), an arabino-based rigid amphipathic fusion inhibitor, targets virion envelope lipids to inhibit fusion of influenza virus, hepatitis C virus, and other enveloped viruses. J. Virol. **87:**3640–3654. http://dx.doi.org/10.1128/JVI.02882-12.
4. **Katz DH, Marcelletti JF, Pope LE, Khalil MH, Katz LR, McFadden R.** 1994. *n*-Docosanol: broad spectrum anti-viral activity against lipid-enveloped viruses. Ann. N. Y. Acad. Sci. **724:**472–488. http://dx.doi.org/10.1111/j.1749-6632.1994.tb38949.x.
5. **Soares MM, King SW, Thorpe PE.** 2008. Targeting inside-out phosphatidylserine as a therapeutic strategy for viral diseases. Nat. Med. **14:**1357–1362. http://dx.doi.org/10.1038/nm.1885.
6. **St. Vincent MR, Colpitts CC, Ustinov AV, Muqadas M, Joyce MA, Barsby NL, Epand RF, Epand RM, Khramyshev SA, Valueva OA, Korshun VA, Tyrrell DL, Schang LM.** 2010. Rigid amphipathic fusion inhibitors, small molecule antiviral compounds against enveloped viruses. Proc. Natl. Acad. Sci. U. S. A. **107:**17339–17344. http://dx.doi.org/10.1073/pnas.1010026107.
7. **Stiasny K, Heinz FX.** 2004. Effect of membrane curvature-modifying lipids on membrane fusion by tick-borne encephalitis virus. J. Virol. **78:**8536–8542. http://dx.doi.org/10.1128/JVI.78.16.8536-8542.2004.
8. **Vigant F, Lee J, Hollmann A, Tanner LB, Akyol Ataman Z, Yun T, Shui G, Aguilar HC, Zhang D, Meriwether D, Roman-Sosa G, Robinson LR, Juelich TL, Buczkowski H, Chou S, Castanho MA, Wolf MC, Smith JK, Banyard A, Kielian M, Reddy S, Wenk MR, Selke M, Santos NC, Freiberg AN, Jung ME, Lee B.** 2013. A mechanistic paradigm for broad-spectrum antivirals that target virus-cell fusion. PLoS Pathog. **9:**e1003297. http://dx.doi.org/10.1371/journal.ppat.1003297.
9. **Wolf MC, Freiberg AN, Zhang T, Akyol-Ataman Z, Grock A, Hong PW, Li J, Watson NF, Fang AQ, Aguilar HC, Porotto M, Honko AN, Damoiseaux R, Miller JP, Woodson SE, Chantasirivisal S, Fontanes V, Negrete OA, Krogstad P, Dasgupta A, Moscona A, Hensley LE, Whelan SP, Faull KF, Holbrook MR, Jung ME, Lee B.** 2010. A broad-spectrum antiviral targeting entry of enveloped viruses. Proc. Natl. Acad. Sci. U. S. A. **107:**3157–3162. http://dx.doi.org/10.1073/pnas.0909587107.
10. **Zasloff M, Adams AP, Beckerman B, Campbell A, Han Z, Luijten E, Meza I, Julander J, Mishra A, Qu W, Taylor JM, Weaver SC, Wong GC.** 2011. Squalamine as a broad-spectrum systemic antiviral agent with therapeutic potential. Proc. Natl. Acad. Sci. U. S. A. **108:**15978–15983. http://dx.doi.org/10.1073/pnas.1108558108.
11. **Melikyan GB.** 2010. Driving a wedge between viral lipids blocks infection. Proc. Natl. Acad. Sci. U. S. A. **107:**17069–17070. http://dx.doi.org/10.1073/pnas.1012748107.
12. **Song JM, Seong BL.** 2010. Viral membranes: an emerging antiviral target for enveloped viruses? Expert Rev. Anti Infect. Ther. **8:**635–638. http://dx.doi.org/10.1586/eri.10.51.
13. **Vigant F, Jung M, Lee B.** 2010. Positive reinforcement for viruses. Chem. Biol. **17:**1049–1051. http://dx.doi.org/10.1016/j.chembiol.2010.10.002.
14. **Wojcechowskyj JA, Doms RW.** 2010. A potent, broad-spectrum antiviral agent that targets viral membranes. Viruses **2:**1106–1109. http://dx.doi.org/10.3390/v2051106.
15. **Costa L, Faustino MAF, Neves MGPMS, Cunha A, Almeida A.** 2012. Photodynamic incativation of mammalian viruses and bacteriophages. Viruses **4:**1034–1074. http://dx.doi.org/10.3390/v4071034.
16. **Chotimarkorn C, Nagasaka R, Ushio H, Ohshima T, Matsunaga S.** 2005. Development of novel fluorescent probe 3-perylene diphenylphosphine for determination of lipid hydroperoxide with fluorescent image analysis. Biochem. Biophys. Res. Comm. **338:**1222–1228. http://dx.doi.org/10.1016/j.bbrc.2005.10.060.
17. **Hirayama J, Ikebuchi K, Abe H, Kwon KW, Ohnishi Y, Horiuchi M, Shinagawa M, Ikuta K, Kamo N, Sekiguchi S.** 1997. Photoinactivation of virus infectivity by hypocrellin A. Photochem. Photobiol. **66:**697–700. http://dx.doi.org/10.1111/j.1751-1097.1997.tb03209.x.
18. **Olivo M, Chin WLW.** 2006. Perylenequinones in photodynamic therapy: cellular versus vascular response. J. Environ. Pathol. Toxicol. Oncol. **25:**223–237. http://dx.doi.org/10.1615/JEnvironPatholToxicolOncol.v25.i1-2.140.
19. **Plaetzer K, Krammer B, Berlanda J, Berr F, Kiesslich T.** 2009. Photophysics and photochemistry of photodynamic therapy: fundamental aspects. Lasers Med. Sci. **24:**259–268. http://dx.doi.org/10.1007/s10103-008-0539-1.
20. **Fernandez JM, Bilgin MD, Grossweiner LI.** 1997. Singlet oxygen generation by photodynamic agents. J. Photochem. Photobiol. B Biol. **37:**131–140. http://dx.doi.org/10.1016/S1011-1344(96)07349-6.
21. **Stachowiak JC, Brodsky FM, Miller EA.** 2013. A cost-benefit analysis of the physical mechanisms of membrane curvature. Nat. Cell Biol. **15:**1019–1027. http://dx.doi.org/10.1038/ncb2832.
22. **Lentz BR.** 1993. Use of fluorescent-probes to monitor molecular order and motions within liposome bilayers. Chem. Phys. Lipids **64:**99–116. http://dx.doi.org/10.1016/0009-3084(93)90060-G.

23. **Idris NM, Gnanasammandhan MK, Zhang J, Ho PC, Mahendran R, Zhang Y.** 2012. In vivo photodynamic therapy using upconversion nanoparticles as remote-controlled nanotransducers. Nat. Med. **18:**1580–1585. http://dx.doi.org/10.1038/nm.2933.
24. **Kharkwal GB, Sharma SK, Huang YY, Dai TH, Hamblin MR.** 2011. Photodynamic therapy for infections: clinical applications. Lasers Surg. Med. **43:**755–767. http://dx.doi.org/10.1002/lsm.21080.
25. **Santos NC, Prieto M, Castanho MA.** 1998. Interaction of the major epitope region of HIV protein gp41 with membrane model systems. A fluorescence spectroscopy study. Biochemistry **37:**8674–8682.
26. **Evans E, Rawicz W.** 1990. Entropy-driven tension and bending elasticity in condensed-fluid membranes. Phys. Rev. Lett. **64:**2094–2097. http://dx.doi.org/10.1103/PhysRevLett.64.2094.
27. **Rawicz W, Olbrich KC, McIntosh T, Needham D, Evans E.** 2000. Effect of chain length and unsaturation on elasticity of lipid bilayers. Biophys. J. **79:**328–339. http://dx.doi.org/10.1016/S0006-3495(00)76295-3.